

The relationship between the crystal structure and optical properties for isomeric aminopyridinium iodobismuthates

Petr A. Buikin,^{a,b} Andrey B. Ilyukhin,^a Alexander E. Baranchikov,^a
Khursand E. Yorov^{a,c} and Vitalii Yu. Kotov^{*a,b,d}

^a N. S. Kurnakov Institute of General and Inorganic Chemistry, Russian Academy of Sciences, 119991 Moscow, Russian Federation. E-mail: vyukotov@gmail.com

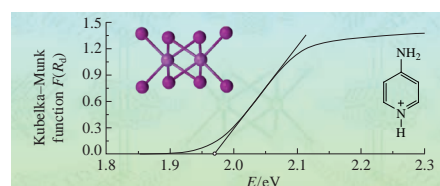
^b Higher Chemical College of the Russian Academy of Sciences, D. I. Mendeleev University of Chemical Technology of Russia, 125047 Moscow, Russian Federation

^c Department of Chemistry, M. V. Lomonosov Moscow State University, 119991 Moscow, Russian Federation

^d National Research University Higher School of Economics, 101000 Moscow, Russian Federation

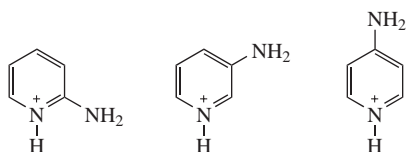
DOI: 10.1016/j.mencom.2018.09.012

The relationship between crystal structures of three isomeric aminopyridinium iodobismuthates containing one-dimensional $[(\text{BiI}_4)_n]^{n-}$ anions, acidity of aminopyridinium cations and optical properties was revealed.

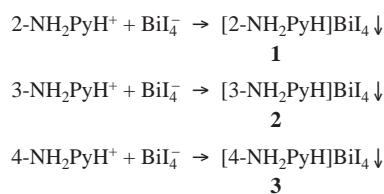


In recent years, the chemistry of organic-inorganic hybrid halobismuthates has attracted growing attention from advanced materials studies. This interest was inspired by promising physical properties, inherent ones of this class of compounds, e.g., semiconductivity, photochromism, luminescence, etc. The crystal structures of hybrid halobismuthates are usually built up by isolated corner-sharing or edge-sharing BiX_6 octahedra which form isolated ionic units, infinite chains, or two dimensional networks.^{1–3} Compounds containing $[(\text{BiX}_5)_n]^{2n-}$ infinite linear anionic chains (with *trans-trans* configuration, X = Br, I) are of particular interest since most of them possess low band gap energies (E_g). However, such compounds are not numerous.^{2,4–9} The most common anionic form of iodobismuthates is the polynuclear anion $[(\text{BiI}_4)_n]^{n-}$.³ Inorganic iodobismuthates containing this anion are represented by potassium, magnesium, manganese and lithium salts.¹⁰ In the case of hybrid tetraiodobismuthates, single and double charged cations can be found in derivatives of aliphatic^{11–13} and aromatic^{14–17} compounds, including aliphatic¹⁸ and aromatic^{19–26} heterocyclic ones. The band gap of such semiconductors is usually higher than that of compounds containing $[(\text{BiI}_5)_n]^{2n-}$. However, these values strongly depend on the nature of the ion interactions inside the crystal, which are determined by the functional groups of the corresponding cation.^{10,18,26} Thus, we believe that these numerous compounds are the good model objects to study the effect of different factors on the band gap values.

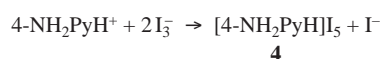
In this work, the most challenging issue was to determine the influence of cation acidity on the structure of the hybrid iodobismuthates and their spectral characteristics. Therefore, 2-, 3- and 4-aminopyridinium iodobismuthates were chosen as the set of objects exhibiting significantly different acidic properties.



The interaction of 2-, 3- and 4-aminopyridinium cations with the iodobismuthate anions in acidified aqueous solutions resulted in the formation of red precipitates **1–3** (for procedures, see Online Supplementary Materials).



Products **1–3** are soluble in DMF and DMSO, slightly soluble in acetonitrile and ethanol, and insoluble in water. All of these compounds are freely soluble in concentrated HI. Drying of the solution of compound **3** in concentrated HI caused a color change of the precipitate as compared to the color of the starting compound **3**. According to the XRD data (Figure S9, Online Supplementary Materials), the obtained product mainly consists of compound **3**, but also contains some unidentified impurities. One of the impurity crystals selected from the mixture turned out to be a black 4-aminopyridinium polyiodide.



Structures of products **1–3**[†] consist of 1D $[\text{BiI}_4]^-$ chains (Figures 1 and S1–S3) and NH_2PyH^+ cations (Figure 2). Compounds **1** and **3** are isostructural. In compound **1**, the cation

[†] Experimental single crystal data were collected on a Bruker SMART APEX2 instrument.³³ The absorption was taken into account by a semi-empirical method based on equivalents using SADABS.³⁴ The structures were determined using a combination of the direct method and Fourier syntheses. The positions of hydrogen atoms were calculated from geometrical considerations. The cation in compound **1** is disordered along the two-fold axis and it has been refined as a rigid body. The cation in compound **2** is disordered in three equally populated positions. Restrictions on the

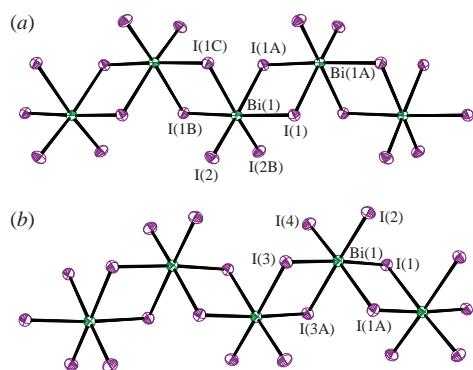


Figure 1 1D-chains in compounds (a) **1** and (b) **2** (the thermal ellipsoids are shown at 50% probability level).

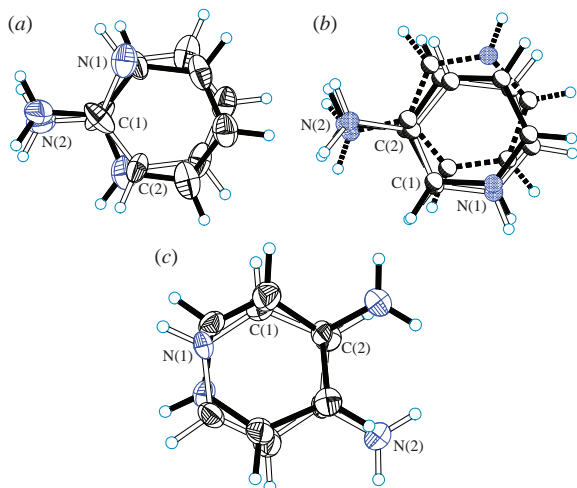


Figure 2 Disordered cations in compounds (a) **1**, (b) **2**, and (c) **4** (the thermal ellipsoids are shown at 50% probability level).

is disordered along the two-fold axis [Figure 2(a)], while in compound **3** the cation has a two-fold crystallographic symmetry. The bismuth atom in products **1** and **3** is located on the two-fold axis, and there is the inversion center between I(1) and I(1A) atoms (see Figure 1). The unshared electron pair of Bi is partially stereochemically active since the Bi(1)–I(1–3) bond lengths are 2.94, 3.08, and 3.25 Å in compound **1** and 2.96,

cation geometry were imposed using the same instruction. The cation in compound **4** is disordered along the two-fold axis. The structures of compounds **1**, **3**, and **4** were refined by the full-matrix anisotropic least squares method. The structure of **2** was refined by the full-matrix anisotropic(Bi,I)-isotropic(C,N) least squares method. All the calculations were carried out using SHELXS and SHELXL software.³⁵

Crystal data for 1. Deep red block (0.2 × 0.12 × 0.08 mm), orthorhombic, space group *Pbcn*, at 150 K: *a* = 11.8999(3), *b* = 15.1567(4) and *c* = 7.6774(2) Å, *V* = 1384.72(6) Å³, *Z* = 4, *d*_{calc} = 3.894 g cm⁻³. Total 17953 reflections were collected (2.176° < *θ* < 30.032°), *μ* = 21.613 mm⁻¹, 2035 independent reflections (*R*_{int} = 0.0408) and 1917 ones with *I* > 2σ(*I*). Data/restraints/parameters are 2035/3/75. The final refinement parameters were: *R*₁ = 0.0267, *wR*₂ = 0.0681 for reflections with *I* > 2σ(*I*); *R*₁ = 0.0287, *wR*₂ = 0.0693 for all reflections; largest difference peak/hole 2.443/–1.486 eÅ⁻³. GOF = 1.118.

Crystal data for 2. Red block (0.3 × 0.2 × 0.16 mm), monoclinic, space group *P2₁/c*, at 150 K: *a* = 7.6660(4), *b* = 14.1101(7) and *c* = 12.9262(6) Å, *β* = 93.2850(10)°, *V* = 1395.90(12) Å³, *Z* = 4, *d*_{calc} = 3.862 g cm⁻³. Total 19544 reflections were collected (2.661° < *θ* < 30.505°), *μ* = 21.440 mm⁻¹, 4244 independent reflections (*R*_{int} = 0.0412) and 3706 ones with *I* > 2σ(*I*). Data/restraints/parameters are 4244/45/130. The final refinement parameters were: *R*₁ = 0.0329, *wR*₂ = 0.0721 for reflections with *I* > 2σ(*I*); *R*₁ = 0.0385, *wR*₂ = 0.0739 for all reflections; largest difference peak/hole 2.241/–2.316 eÅ⁻³. GOF = 1.237.

3.07, and 3.19 Å in compound **3**, respectively (Table S1, Online Supplementary Materials). The BiI₆³⁻ octahedron is distorted leading to the shift of I(1)Bi(1)I(1B) fragment towards the I(2)I(2B) edge. The 2-NH₂PyH⁺ cations are located one below the other, and such a geometry is stabilized by π–π stacking interactions (see Figure S2). Hydrogen bonds (N–H...I) interconnect the structural units forming a 3D framework.

Compound **2** contains 1D [BiI₄]⁻ chains similar to those in **1** and **3**. The short bond lengths for the terminal I atoms in the Bi(1)–I(2,4) moiety are 2.91 Å, the long bonds for the I atoms in transpositions to them in Bi(1)–I(1A,3A) are 3.25 and 3.31 Å, and the medium values are 3.09 and 3.11 Å [Figure 1(b) and Table S1]. The mutual arrangements of structural units in compounds **1–3** are similar (Figures S3 and S4). There are a number of Bi- and Sb-containing halometallates possessing the crystal structures analogous to that of **2** (Table S3).^{12,18,26–29} In compound **4**, the anion I₅⁻ is located on the crystallographic plane *m*, while the cation is disordered along the two-fold axis [Figure 1(c)]. The I₅⁻ anions form a 3D sublattice (Figure S5) with the shortest contacts I...I of 3.81, 3.88 and 3.90 Å. The 4-NH₂PyH⁺ cations are located in the voids of this sublattice (Figure S6).

The diffuse reflectance spectra (DRS)[‡] of compounds **1–3** are shown in Figure S7 as the Kubelka–Munk function vs. light energy:³⁰

$$F(R_d) = \frac{(1 - R_d)^2}{2R_d},$$

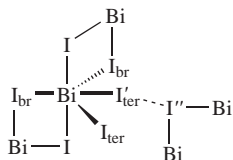
where *R_d* is the absolute reflectance of the sample layer. The optical band gap energies were estimated *via* an extrapolation of the linear parts of corresponding curves to the *F(R_d)* value of 0. The optical band gap values are 2.00 (**1**) and 1.97 eV (**3**). The value obtained for compound **2** (2.07 eV) is not characteristic of it since it is not a single phase product (see Online Supplementary Materials), however this indicates the absence of significant quantities of any compounds having the *E_g* value of less than 2.07 eV in the mixture.

The aminopyridinium cations possess acidic properties, which depend on the position of the substituent on the pyridine ring and decrease through the resonance stabilization typical of 2- and especially 4-aminopyridinium ions. In this case, the charge of the cations is delocalized between the two nitrogen atoms. The p*K_a* values for aqueous solutions increase in the series of 3-NH₂PyH⁺ (6.6) < 2-NH₂PyH⁺ (7.1) < 4-NH₂PyH⁺ (9.1).³¹

Crystal data for 3. Deep red block (0.32 × 0.1 × 0.1 mm), orthorhombic, space group *Pbcn*, at 150 K: *a* = 12.2131(7), *b* = 14.8489(8) and *c* = 7.5997(4) Å, *V* = 1378.21(13) Å³, *Z* = 4, *d*_{calc} = 3.912 g cm⁻³. Total 17680 reflections were collected (2.159° < *θ* < 31.489°), *μ* = 21.715 mm⁻¹, 2227 independent reflections (*R*_{int} = 0.0443) and 2001 ones with *I* > 2σ(*I*). Data/restraints/parameters are 2227/0/57. The final refinement parameters were: *R*₁ = 0.0207, *wR*₂ = 0.0512 for reflections with *I* > 2σ(*I*); *R*₁ = 0.0259, *wR*₂ = 0.0532 for all reflections; largest difference peak/hole 1.510/–1.192 eÅ⁻³. GOF = 1.001.

Crystal data for 4. Black block (0.24 × 0.2 × 0.06 mm), orthorhombic, space group *Pbcm*, at 150 K: *a* = 9.5901(8), *b* = 18.3382(14) and *c* = 7.9508(6) Å, *V* = 1398.27(19) Å³, *Z* = 4, *d*_{calc} = 3.466 g cm⁻³. Total 15817 reflections were collected (2.124° < *θ* < 30.538°), *μ* = 11.085 mm⁻¹, 2270 independent reflections (*R*_{int} = 0.0651) and 1780 ones with *I* > 2σ(*I*). Data/restraints/parameters are 2270/42/94. The final refinement parameters were: *R*₁ = 0.0360, *wR*₂ = 0.0781 for reflections with *I* > 2σ(*I*); *R*₁ = 0.0553, *wR*₂ = 0.0848 for all reflections; largest difference peak/hole 2.443/–1.486 eÅ⁻³. GOF = 1.118.

CCDC 1827677–1827680 contain the supplementary crystallographic data for this paper. These data can be obtained free of charge from The Cambridge Crystallographic Data Centre *via* <http://www.ccdc.cam.ac.uk>.[‡] The reflectance spectra were measured on an Ocean Optics QE65000 spectrophotometer within the frequency range of 11 000–50 000 cm⁻¹ at room temperature.

**Table 1** Selected bond lengths in compounds **1–3**.

Compound	$V/\text{Å}^3$	$r(\text{Bi}-\text{I}_{\text{br}})/\text{Å}$	$r(\text{Bi}-\text{I}'_{\text{ter}})/\text{Å}$	$R(\text{I}'_{\text{ter}}\cdots\text{I}'')/\text{Å}$	E_g/eV
1	1384.7	3.250	2.941	3.940	2.00
2	1395.9	3.311 3.253	2.906 2.914 ^a	3.961 4.167	≥ 2.07
3	1378.2	3.192	2.957	3.919	1.97

^aFor $r(\text{Bi}-\text{I}_{\text{ter}})$.

The charge redistribution significantly affects the geometry of the cation. The C–NH₂ bond in the series of **2** → **1** → **3** shortens from 1.368 to 1.299 Å. The increased positive charge on the amino group in case of 2- and 4-substituted isomers as compared to the 3-substituted one leads to the formation of the stronger hydrogen bonds N–H⋯I (Table S2). Thus, the cations in compounds **1** and **3** are arranged along the *b* axis (see Figure S3) and the cell volume (*V*) corresponding to the same number of formal units is decreased (Table 1). The observed changes confirm the importance of hydrogen bonding upon the structure formation in the hybrid halometallates containing cations with the variable functional groups.³²

The magnitude of interchain I'_{ter}⋯I'' interactions and the Bi–I_{br} distances (I_{ter} is a terminal iodine atom and I_{br} is the bridge-type one) diminishes in the series of **2** → **1** → **3**, while the Bi–I_{ter} distances are elongated in the same order. Thus, the gradual leveling of Bi–I distances occurs in the sequence of **2** → **1** → **3**. Earlier, the similar trend was observed for other hybrid tetraiodobismuthates with a decrease of temperature.^{19,22} At the same time, the decrease of cell volume in the row of **2** → **1** → **3** was accompanied by decrease of E_g values. Thus, the assumption, that the more regular BiI₆³⁻ octahedra form the anionic chain the lower the observed values of the optical band gap, is valid for the series of compounds under investigation.

The weakening of the acidic properties along the row of 3-NH₂PyH⁺ → 2-NH₂PyH⁺ → 4-NH₂PyH⁺ is accompanied by the significant rearrangement of cations due to the resonant stabilization. The increased positive charge on the amino group in case of 4-substituted isomer (as compared to the 3-substituted one) leads to the formation of the stronger hydrogen bonds N–H⋯I. These changes cause the leveling of Bi–I distances along with a decrease in the cell volume and optical band gap values.

In conclusion, new hybrid iodobismuthates containing the isomeric 2-, 3- and 4-aminopyridinium cations have been synthesized and structurally characterized. The effect of amino group position onto the crystal structure and properties of these compounds has been revealed.

This work was carried out within the State Assignment on Fundamental Research to the N. S. Kurnakov Institute of General and Inorganic Chemistry. The authors are grateful to the Center for Collective Use at N. S. Kurnakov Institute of General and Inorganic Chemistry for the opportunity to collect the single crystal X-ray diffraction and X-ray powder diffraction data.

Online Supplementary Materials

Supplementary data associated with this article can be found in the online version at doi: 10.1016/j.mencom.2018.09.012.

References

- Y. Chen, Z. Yang, C.-X. Guo, C.-Y. Ni, Z.-G. Ren, H.-X. Li and J.-P. Lang, *Eur. J. Inorg. Chem.*, 2010, **33**, 5326.
- V. Yu. Kotov, N. P. Simonenko and A. B. Ilyukhin, *Mendeleev Commun.*, 2017, **27**, 454.
- S. A. Adonin, M. N. Sokolov and V. P. Fedin, *Coord. Chem. Rev.*, 2016, **312**, 1.
- V. Yu. Kotov, A. B. Ilyukhin, A. A. Sadovnikov, K. P. Birin, N. P. Simonenko, H. T. Nguyen, A. E. Baranchikov and S. A. Kozyukhin, *Mendeleev Commun.*, 2017, **27**, 271.
- V. Yu. Kotov, A. B. Ilyukhin, K. P. Birin, V. K. Laurinavichyute, A. A. Sadovnikov, Z. V. Dobrokhotova and S. A. Kozyukhin, *New J. Chem.*, 2016, **40**, 10041.
- S. A. Adonin, I. D. Gorokh, A. S. Novikov, P. A. Abramov, M. N. Sokolov and V. P. Fedin, *Chem. Eur. J.*, 2017, **23**, 15612.
- N. Leblanc, N. Mercier, L. Zorina, S. Simonov, P. Auban-Senzier and C. Pasquier, *J. Am. Chem. Soc.*, 2011, **133**, 14924.
- N. Leblanc, N. Mercier, M. Allain, O. Toma, P. Auban-Senzier and C. Pasquier, *J. Solid State Chem.*, 2012, **195**, 140.
- V. Yu. Kotov, A. B. Ilyukhin, A. A. Korlyukov, A. F. Smol'yakov and S. A. Kozyukhin, *New J. Chem.*, 2018, **42**, 6354.
- N. A. Yelovik, A. V. Mironov, M. A. Bykov, A. N. Kuznetsov, A. V. Grigorieva, Z. Wei, E. V. Dikarev and A. V. Shevelkov, *Inorg. Chem.*, 2016, **55**, 4132.
- N. Louvain, N. Mercier and F. Boucher, *Inorg. Chem.*, 2009, **48**, 879.
- S. Chaabouni, S. Kamoun and J. Jaud, *J. Chem. Crystallogr.*, 1997, **27**, 527.
- W. Bi and N. Mercier, *Chem. Commun.*, 2008, 5743.
- M. E. M. Touati, S. Elleuch and H. Boughzala, *Acta Crystallogr.*, 2015, **E71**, 1352.
- S. Pandey, A. P. Andrews and A. Venugopal, *Dalton Trans.*, 2016, **45**, 8705.
- C. Hrizi, N. Chaari, Y. Abid, N. Chniba-Boudjada and S. Chaabouni, *Polyhedron*, 2012, **46**, 41.
- G. A. Bowmaker, P. C. Junk, A. M. Lee, B. W. Skelton and A. H. White, *Aust. J. Chem.*, 1998, **51**, 293.
- A. J. Dennington and M. T. Weller, *Dalton Trans.*, 2016, **45**, 17974.
- M. A. Tershansy, A. M. Goforth, J. R. Gardinier, M. D. Smith, L. Peterson, Jr. and H.-C. zur Loye, *Solid State Sci.*, 2007, **9**, 410.
- B. K. Robertson, W. G. McPherson and E. A. Meyers, *J. Phys. Chem.*, 1967, **71**, 3531.
- Y.-Y. Niu, N. Zhang, H.-W. Hou and S. W. Ng, *Acta Crystallogr.*, 2005, **E61**, 2534.
- A. Gagor, M. Węclawik, B. Bondzior and R. Jakubas, *CrystEngComm*, 2015, **17**, 3286.
- U. Geiser, H. H. Wang, S. M. Budz, M. J. Lowry, J. M. Williams, J. Ren and M.-H. Whangbo, *Inorg. Chem.*, 1990, **29**, 1614.
- H. A. Evans, J. G. Labram, S. R. Smock, G. Wu, M. L. Chabinyk, R. Seshadri and F. Wudl, *Inorg. Chem.*, 2017, **56**, 395.
- A. Cornia, A. C. Fabretti, R. Grandi and W. Malavasi, *J. Chem. Crystallogr.*, 1994, **24**, 277.
- T. Li, Y. Hu, C. A. Morrison, W. Wu, H. Han and N. Robertson, *Sustain. Energy Fuels*, 2017, **1**, 308.
- C. R. Groom, I. J. Bruno and M. P. Lightfoot and S. C. Ward, *Acta Crystallogr.*, 2016, **B72**, 171.
- S. A. Adonin, I. D. Gorokh, P. A. Abramov, P. E. Plyusnin, M. N. Sokolov and V. P. Fedin, *Dalton Trans.*, 2016, **45**, 3691.
- M. Bujak, *Acta Crystallogr.*, 2017, **B73**, 432.
- P. Kubelka and F. Munk, *Z. Tech. Phys.*, 1931, **12**, 593.
- J. A. Joule and K. Mills, *Heterocyclic Chemistry*, 4th edn., Blackwell Science, Oxford, 2002.
- B. Saparov and D. B. Mitzi, *Chem. Rev.*, 2016, **116**, 4558.
- APEX2 and SAINT, Bruker AXS Inc., Madison, Wisconsin, USA, 2007.
- G. M. Sheldrick, *SADABS*, University of Göttingen, Germany, 2014.
- G. M. Sheldrick, *Acta Crystallogr.*, 2015, **C71**, 3.

Received: 12th March 2018; Com. 18/5503